coatings

MDPI

Article

Ultra-Short Pulse HiPIMS: A Strategy to Suppress Arcing during Reactive Deposition of SiO_2 Thin Films with Enhanced Mechanical and Optical Properties

Vasile Tiron [1], Ioana-Laura Velicu [2,*], Teodora Matei [2], Daniel Cristea [3], Luis Cunha [4] and George Stoian [5]

1 Research Department, Faculty of Physics, Alexandru Ioan Cuza University of Iasi, 700506 Iasi, Romania; vasile.tiron@uaic.ro
2 Faculty of Physics, Alexandru Ioan Cuza University of Iasi, 700506 Iasi, Romania; dorateom@yahoo.com
3 Department of Materials Science, Faculty of Materials Science and Engineering, Transilvania University, 500068 Brasov, Romania; daniel.cristea@unitbv.ro
4 Centro de Física, Universidade do Minho, Campus de Gualtar, 4710-057 Braga, Portugal; lcunha@fisica.uminho.pt
5 National Institute of Research and Development for Technical Physics, 700050 Iasi, Romania; gstoian@phys-iasi.ro
* Correspondence: laura.velicu@uaic.ro; Tel.: +40-232-201-199

Received: 4 June 2020; Accepted: 28 June 2020; Published: 30 June 2020

Abstract: In this contribution, based on the detailed understanding of the processes' characteristics during reactive high-power impulse magnetron sputtering (HiPIMS), we demonstrated the deposition of silicon oxide (SiO_2) thin films with improved optical and mechanical performances. A strategy for stabilizing the arc-free HiPIMS of Si target in the presence of oxygen was investigated. Arcing was suppressed by suitable pulse configurations, ensuring good process stability without using any feedback control system. It was found that arcing can be significantly alleviated when ultra-short HiPIMS pulses are applied on the target. The optical and mechanical properties of SiO_2 coatings deposited at various pulsing configurations were analyzed. The coatings prepared by ultra-short pulse HiPIMS exhibited better optical and mechanical performance compared to the coatings prepared by long pulse HiPIMS. The optimized SiO_2 coatings on quartz substrates exhibited an average transmittance of 98.5% in the 190–1100-nm wavelength range, hardness of 9.27 GPa, hardness/Young's modulus ratio of 0.138, and critical adhesion load of 14.8 N. The optical and mechanical properties are correlated with the film morphology, which is inherently related to energetic conditions and process stability during film growth.

Keywords: reactive HiPIMS; silicon oxide; arcing; mechanical properties

1. Introduction

High-power impulse magnetron sputtering (HiPIMS) is a modern technology for physical vapor deposition (PVD) of coatings and thin films, a process where very high power is applied to the target in short unipolar pulses of low duty cycle. The high peak target power density, one of its greatest advantages, facilitates the generation of a high-density plasma where an efficient and significant ionization mechanism of the sputtered target material occurs [1,2]. The high degree of ionization of the plasma leads to an increased ion bombardment of the growing film, which has been proven to be beneficial in the fabrication of coatings exhibiting dense microstructure and excellent adhesion to the substrate [3–5]. Reactive magnetron sputtering was often associated with poisoning of the target and the appearance of hysteresis phenomena, which cause process instability, perturbation, and

very low deposition rate. Due to the high erosion rate during the pulse, and limited target oxidation between the pulses and gas rarefaction effects in front of the target, reactive HiPIMS is efficient in terms of the elimination/suppression of the hysteresis effect, leading to a stable deposition process with a high deposition rate and stoichiometric material transfer from target to substrate [6–10]. Hysteresis phenomena studies were beyond the scope of this paper, considering that the discharge operates in a fully poisoned state. An extensive description of plasma processes and mechanisms of operating the HiPIMS discharge in reactive mode can be found in a tutorial written by Anders [11]. Beside hysteresis behavior, sputtering under poisoned target conditions often results in arcing of the target, and it can produce undesirable macroparticles which can seriously alter the quality of the coatings. Arcing is characterized by a sudden increase in discharge current due to the appearance of small cathode spots on the target, and it is often accompanied by the ejection of microscopic target debris, also known as droplets or macroparticles [12]. Arc prevention should eliminate the ejection of droplets from the target, thus obtaining coatings without structural defects. Due to excessive arcing and hysteresis behavior often experienced in reactive sputtering of Si, it is a real challenge to fabricate high quality silicon oxide (SiO_2) coatings with both excellent optical and mechanical properties. During reactive sputtering of Si, it is very important to suppress arcing, otherwise the process will grow to be even more unstable. The strategy proposed herein, to suppress arcing and to achieve controllable deposition processes in the poisoned target mode, consisted in using very short HiPIMS pulses. A similar strategy was adopted by Hála et al., who succeeded to fabricate SiO_2 thin films in stable reactive deposition conditions by reducing the pulse duration down to 40 µs [13]. In addition, in order to achieve stable deposition conditions, they reduced the target peak power density below 100 W/cm^2, a value much lower than the typical lower limit of HiPIMS discharges (~500 W/cm^2), thus compromising the ion-to-neutral flux ratio. In contrast, the pulsed power supply used in this contribution allows applying very short pulses (down to 3 µs) without compromising the ion-to-neutral flux ratio, the peak power density (estimated over the entire area of the target) exceeding 950 W/cm^2.

The main motivation of this contribution was to investigate the reactive HiPIMS technique, operated in short pulse mode, with the purpose of fabricating high quality SiO_2 coatings with enhanced optical and mechanical performances. To unravel the effect of the process characteristics on the films' properties, SiO_2 thin films were deposited onto quartz and Si (100) substrates, using different HiPIMS pulse durations. The deposited material was selected for its relevance in technological applications. SiO_2 thin films, due their excellent optical and mechanical properties, can be used as protective coatings for durability and performance enhancement of optical surfaces or as optical layer to broaden the functionality of optoelectronic devices. Thanks to their excellent optical performances, SiO_2 films are finding widespread use these days, in microelectronic and optoelectronic applications, including planar waveguide devices [14], optical filters [15], and antireflection coatings [16,17]. Besides good optical properties, suitable mechanical properties such as high hardness, low stress, and good adhesion to the substrate are often the main requirements for the successful use of optical films. Considering that adequate performances of optical coatings depend on the appropriate combination of optical and mechanical properties, a good understanding of the relationship between these properties and the deposition process characteristics is required. In this contribution, the effect of one of the deposition conditions (pulse duration) on the optical and mechanical properties of deposited SiO_2 thin films is highlighted. The samples were analyzed by means of optical transmittance spectroscopy and depth-sensing instrumented indentation, respectively. The scratch resistance and adhesion to the substrate were evaluated by microscratch testing.

2. Materials and Methods

Silicon oxide thin films, with thickness of approximately 1 µm, were deposited on 20 mm × 20 mm quartz, n-type (100) silicon wafer (phosphorus-doped) substrates, and PET foils, at room temperature, by reactive high-power impulse magnetron sputtering (HiPIMS). Quartz was used as substrate for optical properties measurements, while silicon wafers were used as substrate for surface roughness

and mechanical properties measurements. In order to improve the adhesion to the substrate, a silicon nitride (SiN) interlayer (50-nm thick) was deposited by reactive HiPIMS just immediately before SiO_2 thin film deposition, at room temperature, in argon-nitrogen gas mixture, at total pressure of 1 Pa. Preliminary studies have shown that the adhesion critical loads of SiO_2 thin films deposited with SiN interfacial layer is three times higher as compared to SiO_2 thin films deposited without interlayer. The pulse duration and voltage amplitude were set to 5 μs and −900 V, respectively. All experiments were performed in a vacuum deposition system consisting of a stainless-steel chamber, equipped with a 2-inch-diameter circular magnetron and evacuated by a turbomolecular pump to a base pressure of 10^{-5} Pa. The magnetron was loaded with a paramagnetic copper spacer (Cu disc having 50-mm diameter and 3-mm thickness) and with a p-doped (boron) silicon target (99.999% purity, 0.4-mm thickness). The magnetron discharge was operated in pre-ionized pulse mode using a homemade HiPIMS power supply which consisted of a direct current (*dc*) pre-ionizer (for background plasma generation) and a pulse power unit, fed by a *dc* charger power supply. The HiPIMS pulse voltage was set by charger power supply, which was operated in a voltage regulation mode, with a fixed output negative voltage of −700 V. A current limiting resistor of 5 Ω was connected in series with the output of the HiPIMS unit. Due to the delay time between the application of voltage pulse to the magnetron cathode and the beginning of formation of the current pulse, it is difficult to operate the conventional HiPIMS discharge with very short pulse duration. This breakdown delay is related to the time of development of the electron avalanche in the sputtering gas. In order to promote the formation of high-current pulses within a very short time, the sputtering gas was pre-ionized prior to the application of the main voltage pulse to the magnetron cathode. The pre-ionization voltage ensured a low-density plasma (discharge current ~8 mA) near the cathode, which provides a plasma sheath already established before applying the next high-voltage pulse. The presence of the initial background plasma during the pulse-off period significantly reduced the breakdown delay and allowed the generation of fast HiPIMS discharge with very short pulse durations. Moreover, reducing the duration of the voltage pulses resulted in reduced risk of inadvertent arcing [18]. In this work, the average discharge power was kept constant for all experiments at approximately 45 W by changing the pulsing repetition frequency. The peak power reached the value of 18.6 kW, which means a peak power density of 3.2 kW/cm^2 (taking into account that the HiPIMS is a highly non-uniform discharge and the power is mainly dissipated through the target race-track surface area). The depositions were performed by varying the pulse duration from 3 to 10 μs in order to investigate the influence of pulsing configuration on plasma stability and coatings' properties. For pulse durations longer than 10 μs, the HiPIMS discharge was strongly unstable because excessive arcing occurred. Moreover, sputtering the Si target under high power loads and long pulse duration conditions may result in target failure (cracking) due to its poor thermal conductivity and high fragility. It is interesting to note that even for the HiPIMS discharge operated with short pulse duration (3 μs), the peak power value reached 18.6 kW. A mixture of Ar and O_2 gases, at a total pressure of 1 Pa, was used as working gas in all the depositions, with the Ar and O_2 flow rates set to 50 sccm and 5 sccm, respectively. The sample holder was placed in front of the target, at 7-cm distance. A quartz crystal microbalance (QCM), placed near the sample holder, was used for thickness control during the deposition process. The holder was electrically connected to ground. No external substrate heating was applied during the deposition processes and the maximum temperature reached by the substrates did not exceed 60 °C.

The process stability was monitored during the deposition process by means of time-resolved optical emission spectroscopy (TR-OES) using a Jobin Yvonne Triax 550 scanning monochromator (Instruments S.A., Inc., Edison, NJ, USA) with the output on a photo-multiplier tube (PMT) connected to a digital oscilloscope (LeCroy WaveSurfer 424, Iwatsu Test Instruments Corp., Tokyo, Japan) via a 50-ohm resistor. The spectrometer was connected to an UV-Vis-NIR optical fiber equipped with a collimating lens, positioned at a distance of 20 cm from the target's surface, on its axis. In order to obtain the temporal evolution of a certain emission line, the monochromator was set to transmit the wavelength of interest and the voltage across the resistor was recorded as function of time. A wide bandwidth

current probe (Tektronix P6021) and a high-voltage probe (TesTec 1:100), connected to a digital oscilloscope (LeCroy WaveSurfer 424), were used for discharge current and voltage measurements.

The surface topography of selected films deposited on silicon substrates was assessed by atomic force microscopy (AFM) using a NT-MDT Solve Pro instrument (NT-MDT Spectrum Instruments, Moscow, Russia). The crystalline structure of the films deposited on Si substrates was evaluated by X-ray diffractometry (XRD) in θ–2θ configuration using CuKα radiation and a Shimadsu 600 instrument (Shimadsu Corporation, Kyoto, Japan). The optical characterization (transmittance) of the films deposited on quartz substrates was performed using an Evolution 300 UV-Vis-NIR spectrophotometer (Thermo Fisher Scientific, Madison, WI, USA). The hardness (*H*) and elastic modulus (*E*) of the SiO_2 films deposited on Si substrates were evaluated by depth-sensing instrumented indentation (CSM Instruments) using a diamond tip with Berkovich geometry. To minimize the substrate response on the results, the penetration depth was kept below 10% of the coating thickness. The loading and unloading stages (30 s each), separated by a 5-s dwell time (to minimize the creep effect), were applied in accordance to ISO 14577. The data were analyzed using the Oliver and Pharr methodology. The results presented herein were the average of at least 30 indentations per sample. The adhesion/cohesion resistance of the films was characterized by microscratch testing (CSM Instruments) using a standard 100-nm tip radius conical Rockwell diamond tip. The events of interest were the occurrence of cracks in the films, delaminations, and complete film removal. The strain to tensile failure and related cohesive strength of the SiO_2 coatings, as well as their adhesion to the flexible polymer substrate (0.1 mm polyethylene terephthalate—PET foil) were analyzed by means of bending tests.

3. Results and Discussion

3.1. Process Characteristics

Arcing in reactive magnetron sputtering occurs as a consequence of breakthrough of an insulating layer formed on the sputtered target when the charge amount achieves a threshold value [19]. Therefore, the breakdown field appears as a result of charge accumulation, which is strongly related to the energy per pulse. Therefore, a solution to suppress or eliminate arcing is to limit the energy per pulse by limiting the power density and/or pulse duration. Hala et al. succeeded to suppress arcing by drastically limiting the energy per pulse using a peak power density value below 100 W/cm^2 (significantly lower than conventional HiPIMS discharges) and by reducing the pulse duration up to 40 μs [13]. In this contribution, as the peak power density approached 1 kW/cm^2, the strategy adopted to suppress arcing was to further limit the pulse duration by using ultra-short HiPIMS pulse duration (<10 μs). Selected current and voltage waveforms for the reactive HiPIMS discharge operated at various pulse durations (3, 5, and 10 μs) are plotted in Figure 1.

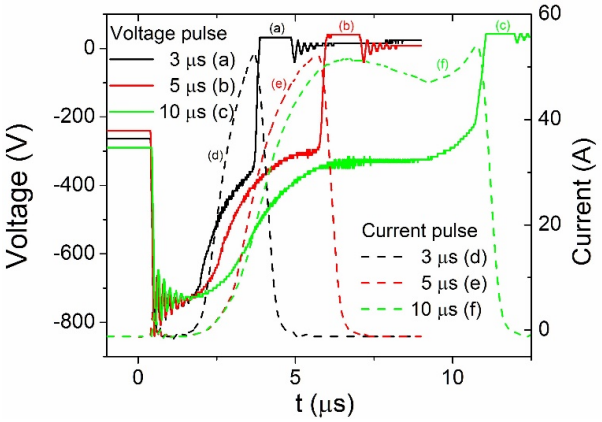

Figure 1. Discharge voltage and current waveforms of reactive HiPIMS deposition of Si target with varying pulse duration.

For each selected pulse duration, the presented data were averaged from 128 measurements, for better comparison. The magnetron discharge was operated in pre-ionized pulsed mode, with a fixed charging voltage of −700 V applied on the HiPIMS power supply input. As the high voltage was applied directly on the magnetron cathode by discharging a capacitor bank, the discharge voltage at the beginning of the pulse exceeded the charging voltage value, initially set to −700 V. Weak oscillations of voltage and current were observed at the beginning of the pulse, during the first 2 μs, most probably as a consequence of the high output inductance of the HiPIMS power supply. During the pulse, the discharge voltage decreased due to ohmic voltage drop on the limiting resistor of 5 ohm, which was connected in series with the output of the HiPIMS unit. For the chosen working gas mixture of Ar/O_2 (50 sccm/5 sccm, respectively) and a total pressure of 1 Pa, self-established pre-ionization voltage values of 240−290 V were attained for the selected pulse durations. The presence of the pre-ionization plasma in the deposition chamber ensured very fast rise time and high replication of the discharge current when a high voltage pulse was applied on the Si cathode. It could be noticed that the discharge ignition resulted in an almost instantaneous current increase, the breakdown delay of the discharge current being lower than 2 μs, while the current decreased to zero, as rapidly as the discharge voltage was switched off. The peak current reached the value of 55 A for all selected pulse durations, indicating the same oxidation state of the Si target surface, regardless of the pulse duration value. It is well known that the secondary electron yield of Si is significantly higher in oxide mode as compared to metal mode [20]. Therefore, the increase of the secondary electron emission coefficient (SEEC), due to the oxygen ion bombardment process, contributed to the discharge current in an oxide mode. The slight increase of the target current, at the end of a long pulse, can be ascribed to the propensity of the discharge for arcing. The steady-state, high-current discharges could be explained by the reactive gas recycling mechanism. The target cleaning phenomenon (target surface composition shift, from more oxidized to less oxidized) and the tendency of the current to decrease were compensated by the reactive gas recycling mechanism: some of the oxygen atoms sputtered from the oxidized target were ionized within the magnetized plasma sheath, after which they were back-attracted to the cathode surface, leading to target surface oxidation and an increase of O^+ ion-induced SEEC [21]. Therefore, the high amplitude of discharge current (55 A), obtained when the Si target was sputtered in oxide mode, was due to the reactive gas recycling mechanism which contributed to the total discharge current through the large fraction of back-attracted O^+ ions and to the increase of the O^+ ion-induced SEEC. This translated into an enhanced ionic and electronic contribution, respectively. To evaluate the process stability under various deposition conditions, the temporal evolution of the intensity of the Ar^+ spectral line (λ = 434.8 nm) was recorded as function of pulse duration. Figure 2 presents the evolution of the selected Ar^+ spectral line for four selected pulse durations (3, 5, 7, and 10 μs).

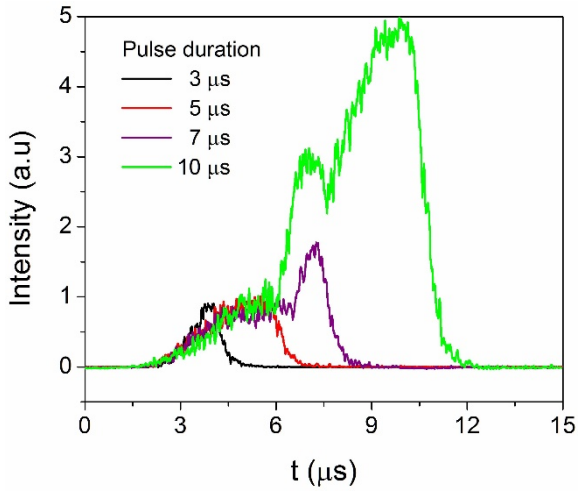

Figure 2. Typical waveforms of Ar^+ (λ = 434.8 nm) spectral line intensity for different pulse durations.

The sudden changes (humps) in Ar^+ spectral line waveforms were related to the occurrence of arcing during the reactive sputtering process. Macro- and microarcs were counted using the recorded waveforms for a cumulative time of 1 min. Therefore, for each selected pulse duration, a total number of Ar+ (λ = 434.8 nm) spectral line waveforms equal to the product of 60 × *f*, where *f* is the pulsing repetition frequency, was recorded. Each recorded waveform was then analysed to identify the occurrence of arcs (the related humps) during the single pulse. Figure 2 shows the occurrence of microarcs (with a lifespan τ = 1 μs) during HiPIMS operation with 7-μs pulse duration and micro- and macroarcs (τ = 2.5 μs) during HiPIMS operation with 10-μs pulse duration. As compared to arc-free discharge, the peak intensity of Ar^+ spectral line during microarcs and macroarcs was 50% and 500% higher, respectively. The arcing rate increased by increasing the pulse duration, this dependency being related to charge accumulation on the target surfaces. The decrease of the pulse duration for a constant average power led to higher pulsing frequency and, thus, to less target poisoning by reactive gas between the pulses, avoiding the arcing of the target. At the same time, shorter pulse duration implied less time for arc development which, in turn, led to a more pronounced arc suppression effect. By using ultra-short pulses, the propensity to arcing was significantly reduced because the arc onset was usually delayed relative to the application of the target voltage. These statements are supported by the study of the arcing rate as a function of the pulse duration, illustrated in Figure 3. It was found that arcing is significantly reduced if the pulse duration decreases below 5 μs.

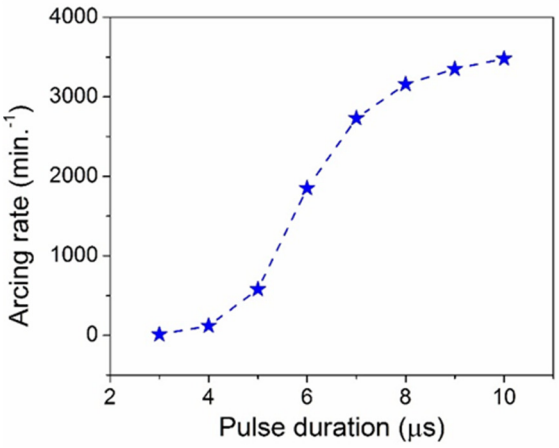

Figure 3. Arcing rate as a function of the pulse duration. Dashed line is used only to guide the eyes.

3.2. Thin Film Characterization

The effect of the deposition process characteristics on the films properties was evaluated by depositing SiO_2 thin films at various HiPIMS pulse durations. The discharge was operated under a constant average target power of 45 W by varying the pulsing frequency. The deposition rate of SiO_2 thin film increased as the pulse duration decreased, due to reduced ion back-attraction effect [22]. Therefore, the deposition rates of the films deposited at 3, 5, and 10 μs were 4.2, 3.7, and 3.2 nm/min., respectively.

3.2.1. Surface Morphology

Figure 4 presents optical micrographs and 2D AFM images of three selected SiO_2 thin films, showing how the pulse duration influences arcs' formation and, implicitly, the surface quality of the deposited samples.

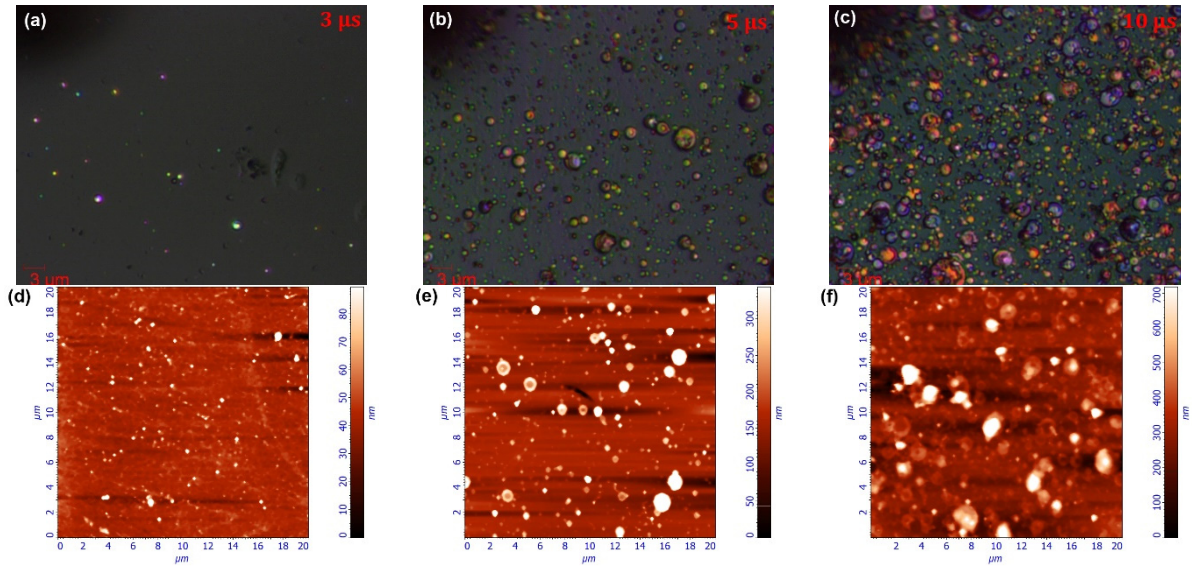

Figure 4. Optical micrographs (**a**–**c**) and AFM images (**d**–**f**) of SiO_2 thin films deposited by reactive HiPIMS for three selected pulse durations (3, 5, and 10 µs).

While the film deposited with a pulse duration of 3 µs showed a smooth and an almost droplet-free surface, increasing the pulse duration up to 10 µs led to the deposition of films with surfaces covered by unwanted droplets and defects, whose topography and texture significantly changed from smooth and fine to rough and coarse. There is no doubt that operating the reactive HiPIMS with ultra-short pulses minimized arcing and improved the quality of the surface of the deposited films. As expected, the AFM results revealed that the pulse duration significantly influenced the surface root mean square (RMS) roughness of the deposited SiO_2 films. The RMS roughness value gradually decreased as the pulse duration decreased, having values of 60.3, 15.0, and 2.0 nm for the films deposited with pulse durations of 10, 5, and 3 µs, respectively. Beyond the suppression of the arcing in reactive HiPIMS by decreasing the pulse duration, these findings can also be ascribed to high-energy ion fluxes, composed of both working gas (positive and negative ions) and sputtered species that arrived at the substrate position during the deposition process [23]. It was demonstrated that in reactive HiPIMS, the negative oxygen ions can gain energies corresponding to the full cathode voltage [24]. The obtained very low surface roughness recommends this technique for fabrication of multi-layer optical stacks for antireflective coating applications. The XRD measurements, not presented here, revealed that all the deposited films were amorphous since the thin films were deposited at room temperature and the crystallization temperature of SiO_2 is higher than 600 °C.

3.2.2. Optical Properties

The optical transmittance, across the 190–1100-nm wavelength range, of ~1-µm-thick SiO_2 thin films deposited on quartz substrates with SiN interlayer, at different pulse durations are shown in Figure 5. The optical transmittance of the SiO_2 thin films showed a significant dependence on the pulse duration, being much lower for the coatings deposited with a longer pulse duration. The average transmittance in the 190–1100-nm wavelength range decreased from 98.5%, for the film deposited with 3-µs pulse, to 49.5%, for the film deposited with 10-µs pulse. The outstanding optical properties (T = 98.5%) of the SiO_2 film deposited at a pulse duration of 3 µs were also confirmed by the optical transmittance of thin film deposited on bare quartz substrate. The transmittance spectra (not shown here) revealed the absence of interference fringes (due to the same refractive index of thin film and substrate, $n \approx 1.5$ at 550 nm) and an average transmittance value of 98.5% in the 190–1100-nm wavelength range. The average transmittance decreased through the haze (scattering) effect [25] caused by the increased surface roughness (from 2.0 to 60.3 nm). The rough surface structure scattered the

incident light at wide angles, resulting in low transmittance in the direction of the detector. The SiO_2 film with high surface roughness enabled an efficient light-trapping process and it can be used to improve the performance of photovoltaic devices.

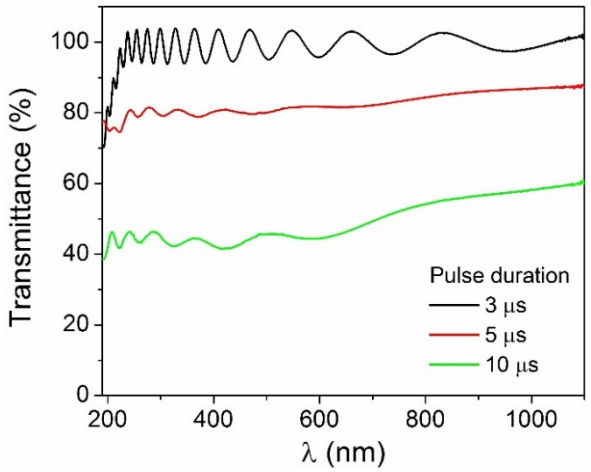

Figure 5. Optical transmittance of SiO_2 thin films deposited by reactive HiPIMS on quartz substrate with 50-nm thick SiN interlayer, for three selected pulse durations.

The experimental results from the optical transmittance and AFM measurements proved that ultra-short HiPIMS provides good process stability and allows the deposition of high-quality optical films, suitable for the fabrication of advanced anti-reflective coatings and optical multilayer stacks.

3.2.3. Mechanical Properties

The mechanical properties of SiO_2 films, deposited on *n*-type (100) silicon substrates, were investigated by instrumented indentation and microscratch tests. The average values of indentation hardness (H), effective Young's modulus (E), H/E and H^3/E^2 ratios, and adhesion critical loads (LCs) are summarized in Table 1. LC1 and LC2 are defined as the load at which the coatings undergo cohesive (LC1) and adhesive (LC2) failure, while LC3 represents the load necessary to remove more than 50% of film from the scratch track. The so-called elastic strain to failure ratio (H/E) is a reliable indicator of wear resistance of materials, with values higher than 0.1 usually indicating a tough coating. The H^3/E^2 ratio is an excellent indicator of a material's resistance against plastic deformation and, generally, values close to 0.05 suggest poor resistance against plastic deformation.

Table 1. Average values of hardness (H), Young's modulus (E), H/E and H^3/E^2 ratios, and cohesion/adhesion critical loads (LC) for SiO_2 films deposited on silicon substrates, using different HiPIMS pulse durations.

τ (μs)	H (GPa)	E (GPa)	H/E	H^3/E^2	LC1 (N)	LC2 (N)	LC3 (N)
3	9.27 ± 0.26	67.35 ± 5.48	0.138	0.176	10.5 ± 0.88	12.2 ± 0.54	14.80 ± 0.42
5	6.51 ± 0.66	85.56 ± 5.32	0.076	0.038	8.50 ±0.85	9.91 ± 0.96	12.00 ± 0.65
10	5.25 ± 0.36	93.10 ± 6.23	0.062	0.020	0.45 ± 0.05	1.14 ± 0.10	5.01 ± 0.53

As it can be seen, the hardness of the deposited SiO_2 films decreased by 43% when the pulse duration increased from 3 to 10 μs. Surprisingly, the effective Young's modulus variation was opposite to that of hardness and its value increased by about 38% when the pulse duration increased. The SiO_2 film deposited at short pulse duration exhibited behavior very close to that of fused silica [26], emphasizing its high packing density. The increasing probable better wear behavior of the SiO_2 films with the decreasing pulse duration was in accordance with both growing hardness and H/E ratio. In general, a good wear resistance is attributed not only to hardness itself, but rather to the H/E

ratio [27]. In this work, the *H*/*E* values varied from 0.062 for the film deposited at pulse duration of 10 µs to 0.138 for the film deposited at 3 µs. The incorporated macroparticles in the film not only acted like defects, but also changed the growth mode from layer by layer to nodule growth [28], leading to nonuniformities in growing films and worse mechanical performances. In order to prove that the SiO_2 film characterized by the highest *H*/*E* ratio showed high elastic strain to failure, the elastic strain to tensile failure and related cohesive strength, as well as the adhesion of 1-µm-thick SiO_2 coating on flexible substrate (PET) were analyzed by means of bending tests. After 100 bending cycles, with radius of curvature of approximately 5 mm, no cracks or delamination events were visible on the SiO_2-coated PET substrate (not shown here). The outstanding optical and mechanical properties resulted in a great potential of this material for applications like flexible displays.

A higher adhesion (higher LC3) for the SiO_2 thin film deposited by using the shortest pulse duration could be associated with low mechanical stress for this film. Such findings can be explained in terms of high-energy particle bombardment (oxygen negative ions). It was demonstrated that even a small amount of highly energetic particles bombarding the film surface can result in a significant reduction of the intrinsic mechanical stress, improving the film's adhesion [29].

4. Conclusions

In this contribution, ultra-short pulse lengths were employed to minimize the probability for the occurrence of arcing during the reactive HiPIMS process. It was shown that arcing can be significantly alleviated when ultra-short HiPIMS pulses are applied on the target. Experimental results revealed that the elimination/suppression of arcing in reactive HiPIMS facilitated the growth of SiO_2 thin films with improved optical and mechanical performances. Improved optical, mechanical, and tribological performances (average transmittance of 98.5% in the 190–1100-nm wavelength range, hardness of 9.27 GPa, *H*/*E* ratio of 0.138, and critical adhesion load of 14.8 N) were obtained when reactive HiPIMS operated with the shortest pulse length (3 µs). Knowledge of appropriate process parameters (pulse duration, in particular) and of the corresponding optical, mechanical, and structural properties will help to optimize the materials and processes for advanced optical applications. The obtained SiO_2 films are very promising for silicon solar cell applications, as good anti-reflective wear protective and absorber layer, as well as for flexible displays.

Author Contributions: Conceptualization, V.T. and I.-L.V.; methodology, V.T. and I.-L.V.; formal analysis, V.T. and I.-L.V.; investigation, V.T., T.M., D.C., G.S., and I.-L.V.; data curation, I.-L.V.; writing—original draft preparation, V.T., I.-L.V., D.C., and L.C.; writing—review and editing, V.T., I.-L.V., D.C., and L.C. All authors have read and agreed to the published version of the manuscript.

Funding: D. Cristea acknowledges the structural funds' project PRO-DD (POS-CCE, O.2.2.1., ID123, SMIS 2637, ctr. no 11/2009) for providing the CSM Instruments infrastructure used for this work.

Conflicts of Interest: The authors declare no conflict of interest.

References

1. Sarakinos, K.; Alami, J.; Konstantinidis, S. High power pulsed magnetron sputtering: A review on scientific and engineering state of the art. *Surf. Coat. Technol.* **2010**, *204*, 1661–1684. [CrossRef]
2. Gudmundsson, J.T.; Brenning, N.; Lundin, D.; Helmersson, U. High power impulse magnetron sputtering discharge. *J. Vac. Sci. Technol. A* **2012**, *30*, 030801. [CrossRef]
3. Velicu, I.-L.; Tiron, V.; Rusu, B.G.; Popa, G. Copper thin films deposited under different power delivery modes and magnetron configurations: A comparative study. *Surf. Coat. Technol.* **2017**, *327*, 192–199. [CrossRef]
4. Tiron, V.; Velicu, I.-L.; Cristea, D.; Lupu, N.; Stoian, G.; Munteanu, D. Influence of ion-to-neutral flux ratio on the mechanical and tribological properties of TiN coatings deposited by HiPIMS. *Surf. Coat. Technol.* **2018**, *352*, 690–698. [CrossRef]
5. Tiron, V.; Velicu, I.-L.; Pana, I.; Cristea, D.; Rusu, B.G.; Dinca, P.; Porosnicu, C.; Grigore, E.; Munteanu, D.; Tascu, S. HiPIMS deposition of silicon nitride for solar cell application. *Surf. Coat. Technol.* **2018**, *344*, 197–203. [CrossRef]

6. Wallin, E.; Helmersson, U. Hysteresis-free reactive high power impulse magnetron sputtering. *Thin Solid Films* **2008**, *516*, 6398–6401. [CrossRef]
7. Aiempanakit, M.; Kubart, T.; Larsson, P.; Sarakinos, K.; Jensen, J.; Helmersson, U. Hysteresis and process stability in reactive high power impulse magnetron sputtering of metal oxides. *Thin Solid Films* **2011**, *519*, 7779–7784. [CrossRef]
8. Surpi, A.; Kubart, T.; Giordani, D.; Tosello, M.; Mattei, G.; Colasuonno, M.; Patelli, A. HiPIMS deposition of TiOx in an industrial-scale apparatus: Effects of target size and deposition geometry on hysteresis. *Surf. Coat. Technol.* **2013**, *235*, 714–719. [CrossRef]
9. Tiron, V.; Sirghi, L. Tuning the band gap and nitrogen content of ZnO_xN_y thin films deposited by reactive HiPIMS. *Surf. Coat. Technol.* **2015**, *282*, 103–106. [CrossRef]
10. Vlček, J.; Belosludtsev, A.; Rezek, J.; Houška, J.; Čapek, J.; Čerstvý, R.; Haviar, S. High-rate reactive high-power impulse magnetron sputtering of hard and optically transparent HfO_2 films. *Surf. Coat. Technol.* **2016**, *290*, 58–64. [CrossRef]
11. Anders, A. Tutorial: Reactive high power impulse magnetron sputtering (R-HiPIMS). *J. Appl. Phys.* **2017**, *12*, 171101. [CrossRef]
12. Anders, A. *Cathodic Arcs: From Fractal Spots to Energetic Condensation*; Springer: New York, NY, USA, 2008.
13. Hála, M.; Vernhes, R.; Zabeida, O.; Klemberg-Sapieha, J.-E.; Martinu, L. Reactive HiPIMS deposition of SiO_2/Ta_2O_5 optical interference filters. *J. Appl. Phys.* **2014**, *116*, 213302. [CrossRef]
14. Rambu, A.; Apetrei, A.; Doutre, F.; Tronche, H.; Tiron, V.; Micheli, M.; Tascu, S. Lithium niobate waveguides with high-index contrast and preserved nonlinearity fabricated by High Vacuum Vapor-phase Proton Exchange. *Photonics Res.* **2020**, *8*, 8–16. [CrossRef]
15. Hinczewski, D.S.; Hinczewski, M.; Tepehan, F.Z.; Tepehan, G.G. Optical filters from SiO_2 and TiO_2 multi-layers using sol–gel spin coating method. *Sol. Energy Mater. Sol. Cells* **2005**, *87*, 181–196. [CrossRef]
16. Raut, H.K.; Nair, A.S.; Dinachali, S.S.; Ganesh, V.A.; Walsh, T.M.; Ramakrishna, S. Porous SiO_2 anti-reflective coatings on large-area substrates by electrospinning and their application to solar modules. *Sol. Energy Mater. Sol. Cells* **2013**, *111*, 9–15. [CrossRef]
17. Kim, K.; Kim, S.; An, S.; Lee, G.-H.; Kim, D.; Han, S. Anti-reflection porous SiO_2 thin film deposited using reactive high power impulse magnetron sputtering at high working pressure for use in a-Si:H solar cells. *Sol. Energy Mater. Sol. Cells* **2014**, *30*, 582–586. [CrossRef]
18. Vašina, P.; Meško, M.; Imbert, J.C.; Ganciu, M.; Boisse-Laporte, C.; de Poucques, L.; Touzeau, M.; Pagnon, D.; Bretagne, J. Experimental study of a pre-ionized high power pulsed magnetron discharge. *Plasma Sources Sci. Technol.* **2007**, *16*, 501–510. [CrossRef]
19. Belkind, A.; Freilich, A.; Scholl, R. Using pulsed direct current power for reactive sputtering of Al_2O_3. *J. Vac. Sci. Technol. A* **1999**, *17*, 1934. [CrossRef]
20. Wittmaack, K. Ion-induced electron emission as a means of studying energy- and angle-dependent compositional changes of solids bombarded with reactive ions: I. Oxygen bombardment of silicon. *Surf. Sci.* **1999**, *419*, 249. [CrossRef]
21. Aiempanakit, M.; Aijaz, A.; Lundin, D.; Helmersson, U.; Kubart, T. Understanding the discharge current behavior in reactive high power impulse magnetron sputtering of oxides. *J. Appl. Phys.* **2013**, *113*, 133302. [CrossRef]
22. Tiron, V.; Velicu, I.; Vasilovici, O.; Popa, G. Optimization of deposition rate in HiPIMS by controlling the peak target current. *J. Phys. D Appl. Phys.* **2015**, *48*, 495204. [CrossRef]
23. Dinca, P.; Tiron, V.; Mihaila, I.; Velicu, I.-L.; Porosnicu, C.; Butoi, B.; Velea, A.; Grigore, E.; Costin, C.; Lungu, C.P. Negative ion-induced deuterium retention in mixed W-Al layers co-deposited in dual-HiPIMS. *Surf. Coat. Technol.* **2019**, *363*, 273–281. [CrossRef]
24. Bowes, M.; Poolcharuansin, P.; Bradley, J.W. Negative ion energy distributions in reactive HiPIMS. *J. Phys. D Appl. Phys.* **2012**, *46*, 045204. [CrossRef]
25. Kanniah, V.; Grulke, E.A.; Druffel, T. The effects of surface roughness on low haze ultrathin nanocomposite films. *Thin Solid Films* **2013**, *539*, 170–180. [CrossRef]
26. Schuh, C.A.; Packard, C.E.; Lund, A.C. Nanoindentation and contact mode imaging at high temperatures. *J. Mater. Res.* **2006**, *21*, 725–736. [CrossRef]
27. Leyland, A.; Matthews, A. On the significance of the *H*/*E* ratio in wear control: A nanocomposite coating approach to optimised tribological behaviour. *Wear* **2000**, *246*, 1–11. [CrossRef]

28. Drescher, D.; Koskinen, J.; Scheibe, H.-J.; Mensch, A. A model for particle growth in arc deposited amorphous carbon films. *Diam. Relat. Mater.* **1998**, *7*, 1375. [CrossRef]
29. Bilek, M.M.M.; McKenzie, D.R. A comprehensive model of stress generation and relief processes in thin films deposited with energetic ions. *Surf. Coat. Technol.* **2006**, *200*, 4345–4354. [CrossRef]